



## Original Article

## Effect of rare earth dopants on the radiation shielding properties of barium tellurite glasses

P. Vani<sup>a</sup>, G. Vinitha<sup>a</sup>, M.I. Sayyed<sup>b,c</sup>, Maha M. AlShammari<sup>d</sup>, N. Manikandan<sup>a,\*</sup><sup>a</sup> Division of Physics, School of Advanced Sciences, Vellore Institute of Technology, Chennai, 600127, India<sup>b</sup> Department of Physics, Faculty of Science, Isra University, Amman, Jordan<sup>c</sup> Department of Nuclear Medicine Research, Institute for Research and Medical Consultations (IRMC), Imam Abdulrahman Bin Faisal University (IAU), P.O. Box 1982, Dammam, 31441, Saudi Arabia<sup>d</sup> Computational Unit, Department of Environmental Health, Institute for Research and Medical Consultations (IRMC), Imam Abdulrahman Bin Faisal University, Dammam, 31441, Saudi Arabia

## ARTICLE INFO

## Article history:

Received 4 March 2021

Received in revised form

6 June 2021

Accepted 7 June 2021

Available online 12 June 2021

## Keywords:

Tellurite glasses

Rare earth dopants

Radiation shielding

Linear attenuation coefficient

Half value layer

## ABSTRACT

Rare earth doped barium tellurite glasses were synthesised and explored for their radiation shielding applications. All the samples showed good thermal stability with values varying between 101 °C and 135 °C based on dopants. Structural properties showed the dominance of matrix elements compared to rare earth dopants in forming the bridging and non-bridging atoms in the network. Bandgap values varied between 3.30 and 4.05 eV which was found to be monotonic with respective rare earth dopants indicating their modification effect in the network. Various radiation shielding parameters like linear attenuation coefficient, mean free path and half value layer were calculated and each showed the effect of doping. For all samples, LAC values decreased with increase in energy and is attributed to photoelectric mechanism. Thulium doped glasses showed the highest value of 1.18 cm<sup>-1</sup> at 0.245 MeV for 2 mol.% doping, which decreased in the order of erbium, holmium and the base barium tellurite glass, while half value layer and mean free paths showed an opposite trend with least value for 2 mol.% thulium indicating that thulium doped samples are better attenuators compared to undoped and other rare earth doped samples. Studies indicate an increased level of thulium doping in barium tellurite glasses can lead to efficient shielding materials for high energy radiation.

© 2021 Korean Nuclear Society, Published by Elsevier Korea LLC. This is an open access article under the CC BY-NC-ND license (<http://creativecommons.org/licenses/by-nc-nd/4.0/>).

## 1. Introduction

Radiation sources/facilities have been on the rise for the past few decades which encompasses with that a possible health risk to the personnel involved in its usage and application. Health risks include external disfiguration to internal cell mutations leading to genetic deficiencies. Hence, there is definitely a need to protect the living species from the dangers of exposure to radiation. Conventionally, lead based materials have been used as shielding materials, which due to their inherent drawbacks like toxicity had led researchers towards finding new materials as replacement for these lead-based systems [1–7].

One of the important criteria for shielding materials is that they should possess higher absorption cross section. Glasses are one

important family of materials which have been explored for these applications owing to their stability, density, compositional durability, ease of synthesis etc. Among various glasses, heavy metal oxide doped tellurites have been explored in recent times for shielding applications due to their higher density which is one of the criteria for shielding materials [8–15]. These glasses are found to have better chemical resistance, higher dielectric constant, lower melting temperature etc., which all aids in their applications as shielding materials. Barium/Bismuth doped heavy metal oxide glasses with larger densities have been found to have higher radioactive resistance and showed better shielding characteristics depending on the increasing concentrations of these bismuth/barium dopants [16–19].

Among the heavy metal oxide glasses, barium doped tellurite glasses have been shown to exhibit good thermal and photonic properties leading to probable applications in the fields of Raman gain amplifiers and optical fibers [20]. These barium tellurite glasses have also been shown to exhibit mean free path values

\* Corresponding author.

E-mail address: [manikandan.narendran@vit.ac.in](mailto:manikandan.narendran@vit.ac.in) (N. Manikandan).

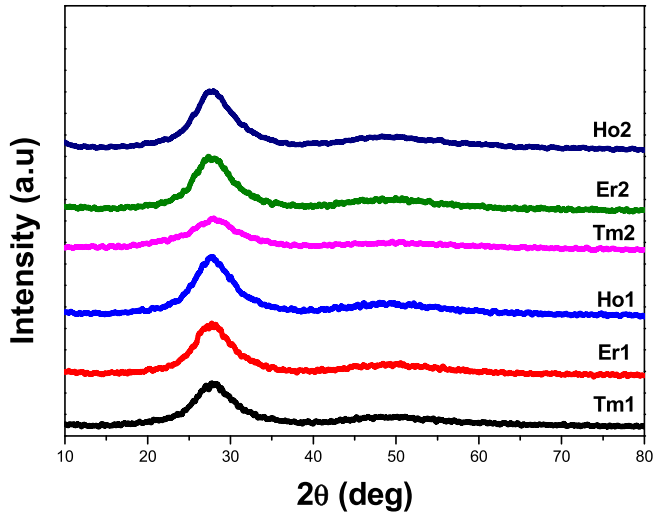


Fig. 1. XRD Patterns of Rare earth doped barium tellurite glasses.

less than standard shielding materials indicating their utilization as better shielding materials [21]. Various modifications in the base barium tellurite glass matrix have also been reported with moderate fluorine doping improving the Raman gain coefficients and also decreasing the absorption due to hydroxyl groups in the samples [22]. Barium tellurite glasses in the form of fluorotellurite had shown higher concentrations of barium leading to yield superior radiation shielding properties [10].

Doping of rare earth oxides helps in improving the densities of these glasses along-with their thermal properties and network structure. And the fundamental nature of tellurite glasses allows doping of these rare earth ions in higher concentrations which are defined by the final applications [1,23,24]. These rare earth dopants have efficient absorption-emission properties of EM radiation in wide wavelength regions. But rare earth doped glasses have not been sufficiently explored for radiation shielding properties. There

have been few reports exclusively on shielding applications of rare earth doped tellurites, some of which are given below. Doping of Samarium oxide in tellurites have been shown to increase the linear attenuation coefficient at all energies [25]. Effect of europium doping in borotellurite glass matrix on the radiation shielding properties have been explored by Rammah et al. [26]. Effect of erbium doping in tellurite glasses in the medical diagnostic energy range has been reported by Tijani et al. [27]. Bismuth barium telluroborate glasses have been found to show higher shielding capability when doped with larger quantities of erbium oxide [28].

In the present work, barium tellurite glasses with 20 mol.% of barium have been used as the host glass. The host was doped with two different concentrations of erbium oxide, holmium oxide and thulium oxide respectively and their basic physical, structural and thermal properties have been explored. Radiation shielding properties of these samples have been calculated and the obtained results have been analysed to predict the better rare earth dopant in the present thermally stable tellurite glass matrix.

## 2. Materials and methods

Glass samples were synthesised using standard melt quenching technique. High purity (Sigma-Aldrich, 99.99%) chemicals were weighed for a total of 10 g, ground, mixed thoroughly and placed in a platinum crucible. Mixed powders were melted at 850 °C for 60 min and then quenched in a preheated brass mould. As-quenched samples were annealed at 290 °C for 300 min to remove the internal stresses. Samples were then allowed to cool to room temperature after which they were cut and polished for further characterisations. Sample compositions synthesised were based on the tie-line 60TeO<sub>2</sub>– 20ZnO–4BaF<sub>2</sub>–(16-x) BaCO<sub>3</sub>-xRE where RE- Tm<sub>2</sub>O<sub>3</sub>, Er<sub>2</sub>O<sub>3</sub>, Ho<sub>2</sub>O<sub>3</sub> and x = 1 & 2.

The sample code and compositions are as mentioned below.

60TeO<sub>2</sub>– 20ZnO– 4BaF<sub>2</sub>– 16BaCO<sub>3</sub> - TZBB.

60TeO<sub>2</sub>– 20ZnO– 4BaF<sub>2</sub>– 15BaCO<sub>3</sub>– 1Tm<sub>2</sub>O<sub>3</sub> - TZBBTm1.0.

60TeO<sub>2</sub>– 20ZnO– 4BaF<sub>2</sub>– 15BaCO<sub>3</sub>– 1Er<sub>2</sub>O<sub>3</sub> - TZBBEr1.0.

60TeO<sub>2</sub>– 20ZnO– 4BaF<sub>2</sub>– 15BaCO<sub>3</sub>– 1Ho<sub>2</sub>O<sub>3</sub> - TZBBHo1.0.

60TeO<sub>2</sub>– 20ZnO– 4BaF<sub>2</sub>– 14BaCO<sub>3</sub>– 2Tm<sub>2</sub>O<sub>3</sub> - TZBBTm2.0.

Table 1

Various physical properties and thermal stability of rare earth doped barium tellurite glasses.

Sample Code	Molecular weight of RE (g/mol)	Average Molecular weight (g/mol)	Density (g/cm <sup>3</sup> )	Molar volume (cm <sup>3</sup> /mol)	Band gap (eV)	Thermal Stability (°C)
TZBB	—	150.62	5.402	27.88	3.615	135 [21]
TZBBHo1.0	377.86	152.42	5.448	27.97	4.020	121
TZBBHo2.0	—	154.23	5.486	28.11	3.964	122
TZBBEr1.0	382.56	152.47	5.466	27.89	3.964	114
TZBBEr2.0	—	154.32	5.513	27.98	4.051	117
TZBBTm1.0	385.87	152.50	5.473	27.86	3.300	101
TZBBTm2.0	—	154.39	5.518	27.97	3.573	119

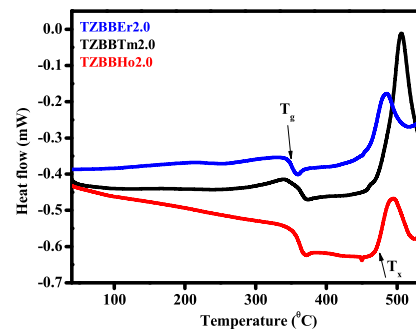
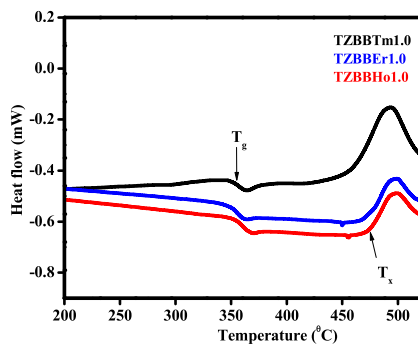
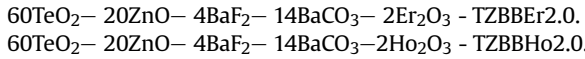


Fig. 2. DSC Patterns of Rare earth doped barium tellurite glasses.



Rigaku X-Ray diffractometer with Cu-K $\alpha$  radiation (1.54 Å) was utilized to record the XRD pattern of these glasses between 20 and 80°. Density of the samples was measured using Archimedes principle in distilled water (immersion liquid) with an accuracy of 0.001 g/cm<sup>3</sup>. Thermal Analysis was done using Metler-Toledo differential scanning calorimeter under Argon atmosphere. 20–30 mg of powder samples were taken in a crucible and then heated from ambient up to 550 °C at a heating rate of 10 °C/min. Raman spectra of the glasses were measured with Nd:YAG laser (532 nm) as the excitation source. Evolution 300, UV–Vis spectrophotometer was used to measure the absorption spectra in the wavelength range of 200–800 nm. On the other hand, the radiation shielding attributes for the synthesised TZBB-X glasses were determined between 0.245 and 1.41 MeV, by generating the Phy-X computer program [2].

### 3. Results and discussion

Amorphous nature of the samples was confirmed from the X-Ray diffraction measurements. All the samples showed a broad

hump indicating the absence of any crystallinity in these samples. Representative diffractogram is given in Fig. 1.

#### 3.1. Physical properties

Measured physical parameters like density and calculated molar volume values showed an increase with all the dopant concentrations (Table 1). Density of base glass was measured to be 5.402 g/cm<sup>3</sup>. As these samples were initially doped with 1 mol.% and 2 mol.% of holmium oxide, density of the samples increased to 5.448 and 5.486 g/cm<sup>3</sup> respectively. Similar increase was observed for oxides of both erbium and thulium doping also. This increase which depends on parameters like coordination number, interstitial lattice spacing etc., has been attributed to the heavier mass of the rare earth dopant atoms replacing the lighter barium atoms in the matrix [29]. It could be noted that the ionic radii of these rare earth dopants are in increasing order of thulium (0.880 Å) > erbium (0.890 Å) > holmium (0.901 Å), which are still smaller than that of barium (1.35 Å). As the network barium oxide gets replaced by these rare earth oxides, owing to their smaller sizes, dense filing of void spaces takes place leading to a consequent increase in density and hence compactness of the network as reported earlier [20].

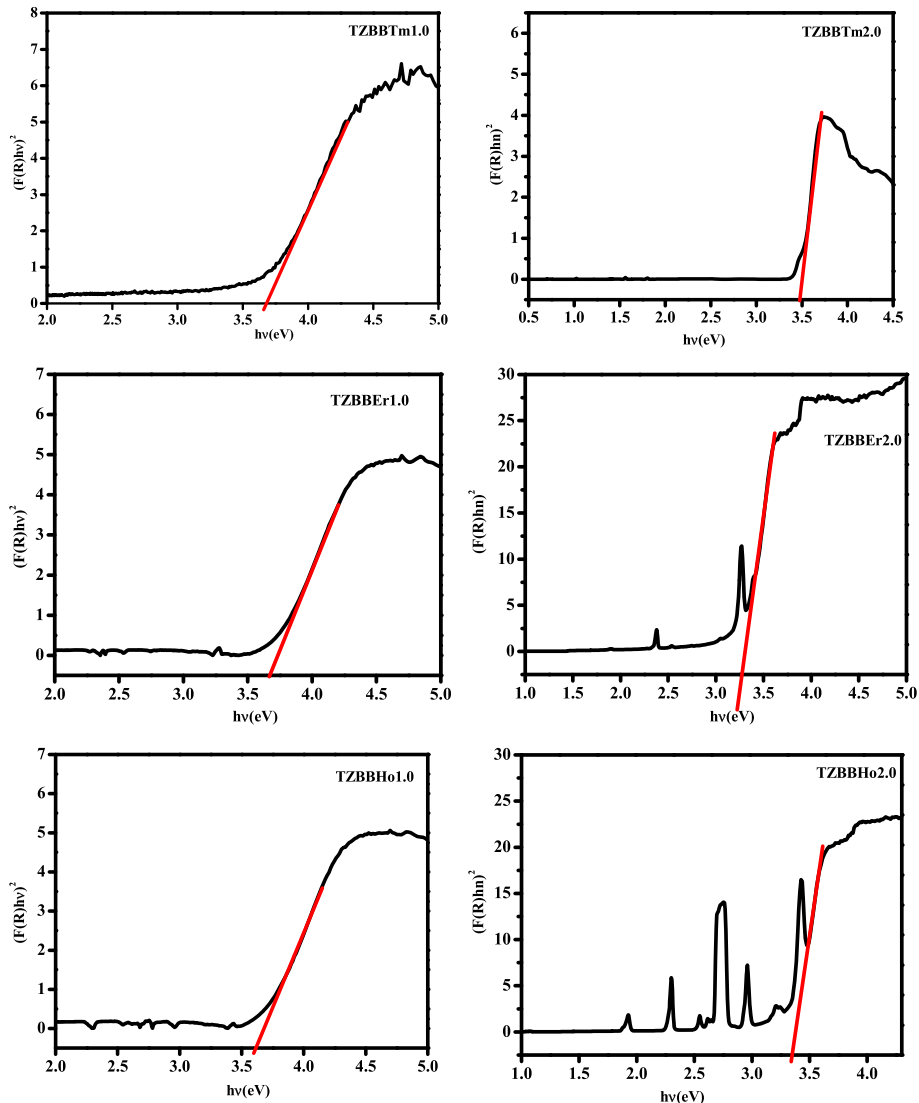


Fig. 3. Tauc Plots of Rare earth doped barium tellurite glasses.

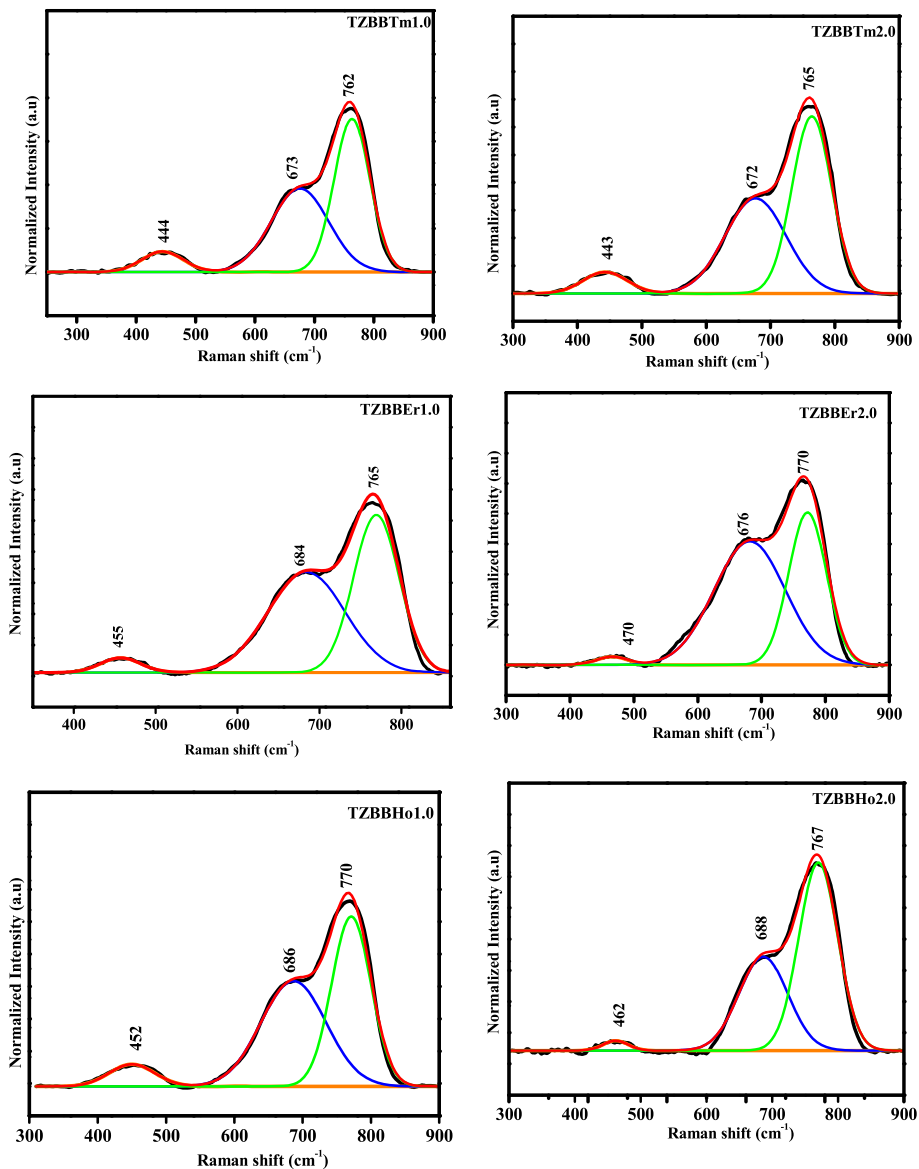


Fig. 4. Raman Spectra of Rare earth doped barium tellurite glasses.

Among the various dopants, owing to the higher mass of thulium oxide, sample doped with lower radii thulium oxide showed the highest density values compared to other dopants and the increase was in the order of thulium oxide > erbium oxide > holmium oxide.

3.2. Thermal properties

Rare earth doped barium tellurite glasses have been subjected to thermal analysis and their thermal parameters like glass transition temperature and peak crystallization temperature were measured from which the thermal stability of the samples was calculated. Measurements were within an accuracy of ±2 °C. As seen from Fig. 2, all these samples showed a single glass transition and crystallization temperatures within the limits of measurement. Measured glass transition temperatures of these samples were found to be around 350 °C as like the base TZBB sample reported earlier [20]. Variations seen in the measured transition temperatures between different concentrations of rare earth dopants is

attributed to the inherent nature of dopant atoms. All these glasses were found to be thermally stable with thermal stability beyond 100 °C indicating that they can withstand thermal cycling below their crystallization temperature without losing their intrinsic glassy nature. This stability indicates that the glasses can also be used in fiber amplifier applications along with the radiation shielding applications explored in this paper.

3.3. Optical properties

Optical bandgap of these materials was calculated from the absorbance spectra measured in the UV–Vis region, which indicated the amorphous nature of these samples with absence of any sharp edges. Mott-Davis relation as given below was utilized to calculate the bandgap of these materials,

$$\alpha(\nu) h\nu = B (h\nu - E_g)^{1/2} \dots \dots \dots (1)$$

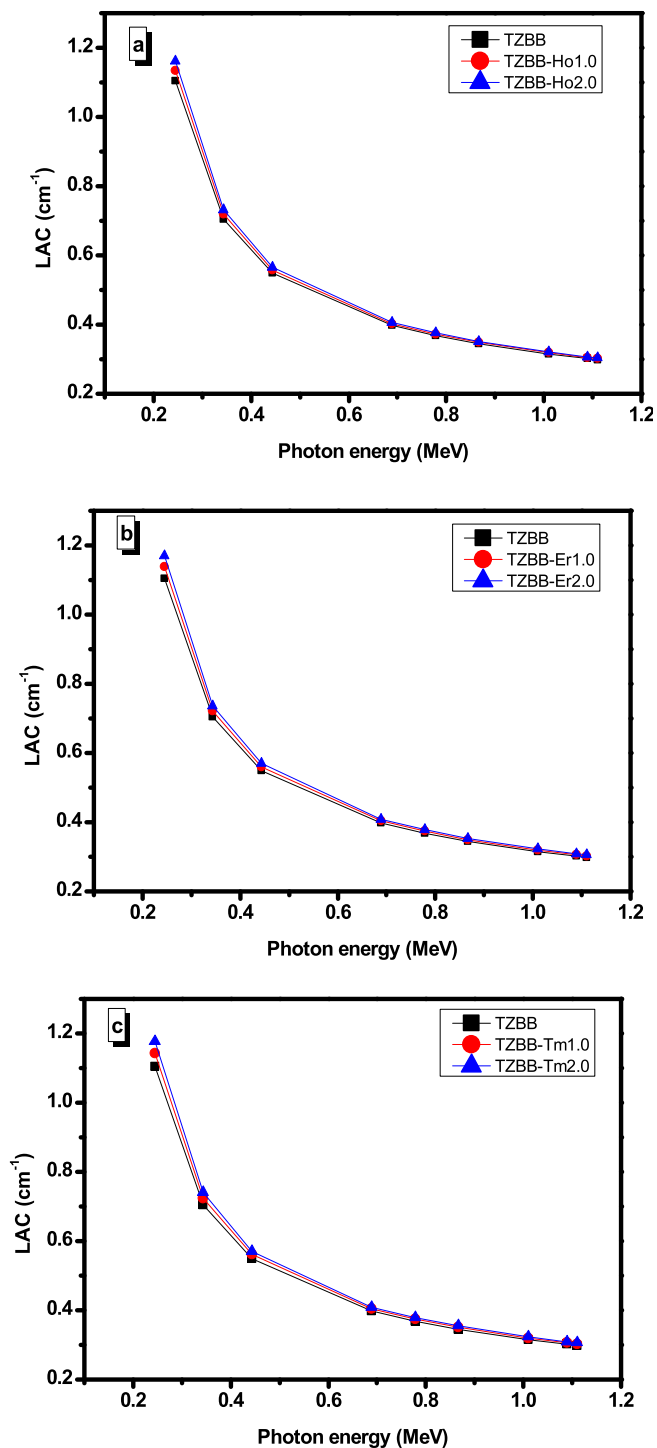


Fig. 5. Linear attenuation coefficient for the prepared glasses.

where the value of  $n$  decides the direct or indirect bandgap [30]. Fig. 3 shows the Tauc's plot for indirect transition in rare earth doped glass samples [31]. The calculated indirect bandgap value for base sample was found to be 3.615 eV, which increased or decreased with erbium/holmium or thulium doping respectively and is shown in Table 1. It could be observed that an increment in holmium concentration from 1 to 2 mol% led to a decrease in bandgap values, while an increase in erbium and thulium

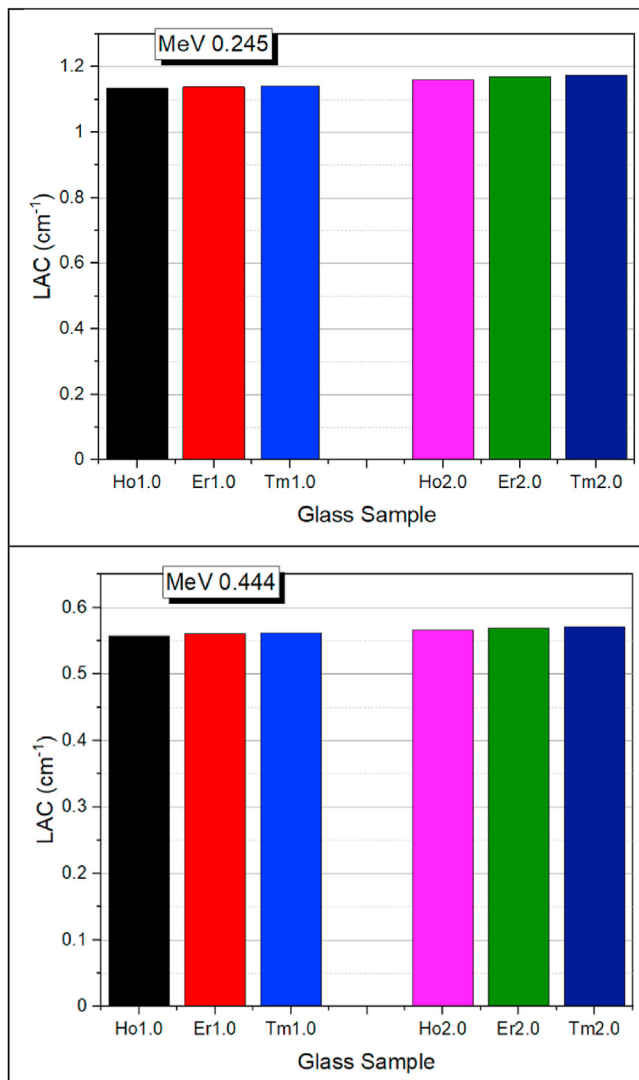


Fig. 6. Linear attenuation coefficient for the Ho1.0, Er1.0 and Tm1.0 (and for the samples with 2 mol% of rare earth ions) at 0.245 and 0.444 MeV.

concentrations led to an increase in bandgap values. The observed changes in bandgap values can be correlated to the presence/absence of bridging and non-bridging oxygen sites, that are affected by the dopants ability to modify the network. Nevertheless, all the samples showed a monotonic change with doping concentration indicating the structural modifications affecting the bandgap values due to doping with rare earth ions [32].

### 3.4. Raman Spectroscopy

Structure of these glasses were studied from Raman spectra measured in the range of 200–1000  $\text{cm}^{-1}$ . All the samples showed three dominant peaks around 450, 670 and 760  $\text{cm}^{-1}$  (Fig. 4). Band around 450  $\text{cm}^{-1}$  corresponds to the bending modes of Te–O–Te. Bands around 670 and 760  $\text{cm}^{-1}$  correspond to the formation of bridging and non-bridging oxygen atoms in the network respectively. Two  $\text{TeO}_4$  trigonal bipyramidal units linked by an oxygen atom form the basic building block of tellurite glass network. Based on the previous report, it could be understood that presence of

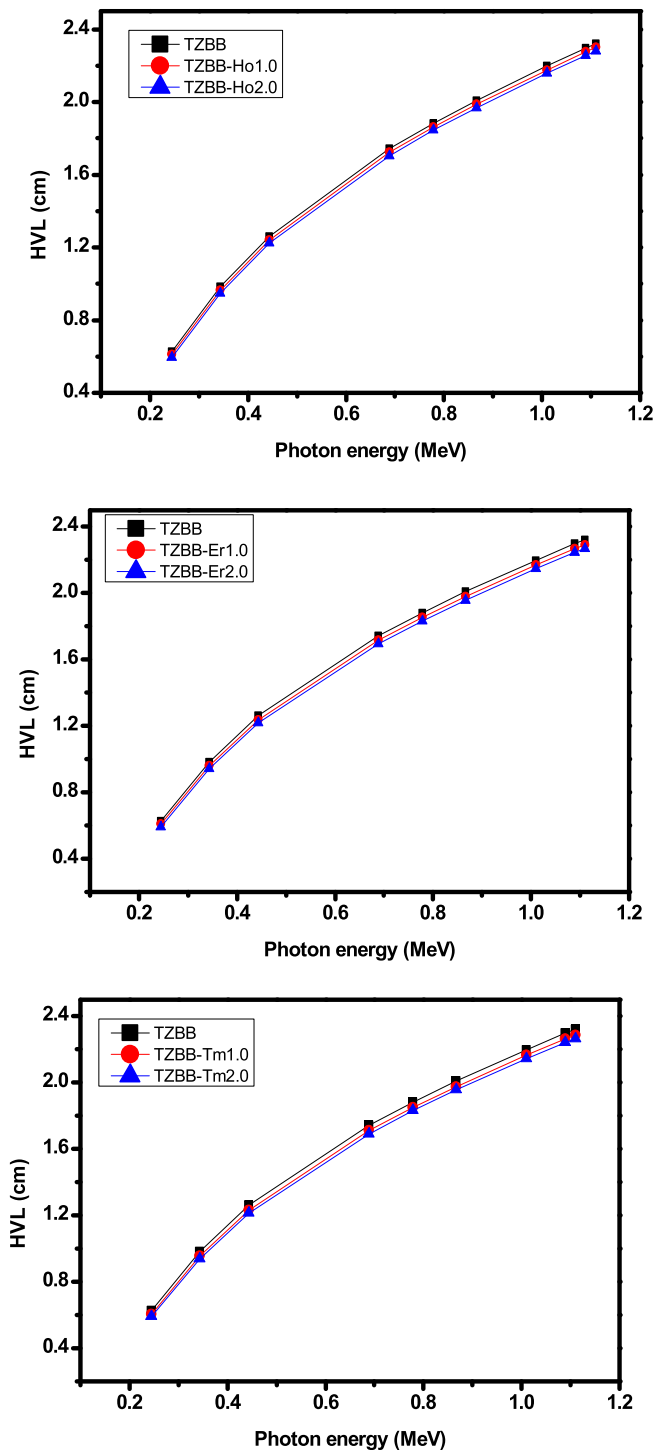


Fig. 7. Half value layer for the fabricated glasses.

Barium oxide leads to modification of the tellurite network causing structural transition from  $TeO_4$  to  $TeO_3$  and  $TeO_{3+\delta}$  units in the base tellurite glass [20]. This is indicated by the presence of dominant peak at  $760\text{ cm}^{-1}$  that corresponds to the formation of non-bridging oxygen atoms in the network which also acts as the predominant sites for rare earth incorporation in a glass matrix [33].

### 3.5. Radiation shielding features

The theoretical linear attenuation coefficient (LAC) determined

by Phy-X software [2] in the energy range of 0.245 MeV up to 1.11 MeV for the TZBB, TZBB-Ho1.0, TZBB-Er1.0, TZBB-Tm1.0, TZBB-Ho2.0, TZBB-Er2.0 and TZBB-Tm2.0 glasses is given in Fig. 5. In order to study the influence of the  $Ho_2O_3$ ,  $Er_2O_3$  and  $Tm_2O_3$  on the LAC, we plotted the LAC for TZBB, TZBB-Ho1.0 and TZBB-Ho2.0 in Fig. 5-a, while we presented the LAC for the TZBB glass and the glasses with 1, 2 mol% of  $Er_2O_3$  in Fig. 5-b and for the TZBB glass and the glasses with 1, 2 mol% of  $Tm_2O_3$  in Fig. 5-c. For the fabricated base sample of barium tellurite glass (i.e. TZBB) and the rare earth ion doped samples, the variation in LAC with the energy was found to be almost identical. All the samples showed a decreasing behaviour in LAC. The trend observed for the LAC is related to the basic processes characterizing the interaction between the radiation and the shielding material [34,35]. Apparently, all the samples have the maximum LAC at 0.245 MeV ( $1.105\text{ cm}^{-1}$  for TZBB) and then LAC reduces drastically. For example, between 0.245 and 0.344 MeV, the LAC reduces from  $1.105$  to  $0.704\text{ cm}^{-1}$  (for TZBB) and from  $1.134$  to  $0.719\text{ cm}^{-1}$  (for TZBB-Ho1.0). Similar trend was observed for the remaining glasses. The current behaviour in LAC maybe explained by photoelectric mechanism, where the possibility of occurrence of this mechanism can be simply written as:

$$\tau \propto \frac{Z^m}{E^3} \tag{2}$$

In the above relation,  $m$  takes values between 4 and 5. This denotes that the probability of this process to occur is high for the photons with low energy.

Moreover, all the fabricated samples own nearly the same LAC between 1.01, 1.09 and 1.11 MeV. This suggests that for  $1.01\text{ MeV} < E < 1.11\text{ MeV}$  the attenuation capability for the fabricated glasses depends weakly upon the composition. Between these energies, Compton scattering is the crucial mode of interaction and the probability for this mode is independent of the attenuator's atomic number [36]. For example, the LAC values for TZBB, TZBB-Ho1.0, TZBB-Er1.0 and TZBB-Tm1.0 at 1.11 MeV are  $0.298$ ,  $0.301$ ,  $0.302$  and  $0.303\text{ cm}^{-1}$  respectively.

Also, the rare earth ions ( $Ho_2O_3$ ,  $Er_2O_3$  and  $Tm_2O_3$ ) increased the LAC values and the samples with any concentration of these rare earth ions have higher LAC than that of the fabricated base sample of barium tellurite glass (i.e. TZBB). From Fig. 5-a, the LAC follows the trend of  $TZBB-Ho2.0 > TZBB-Ho1.0 > TZBB$ . The same is observed in Fig. 5-b, namely the LAC follows the trend of  $TZBB-Er2.0 > TZBB-Er1.0 > TZBB$ , and from Fig. 5-c,  $TZBB-Tm2.0 > TZBB-Tm1.0 > TZBB$ . This can be explained according to the fact that the TZBB has lower density than the samples with  $Ho_2O_3$ ,  $Er_2O_3$  and  $Tm_2O_3$ . In order to compare the effect of the three rare earth ions ( $Ho_2O_3$ ,  $Er_2O_3$  and  $Tm_2O_3$ ) on the LAC values, we plotted the LAC for TZBB-Ho1.0, TZBB-Er1.0 and TZBB-Tm1.0 at two energies 0.245 and 0.444 MeV in Fig. 6. Also, we present the LAC at these two energies for the glasses with 2 mol% of each of the rare earth ions. It is clear that the glass with  $Tm_2O_3$  has higher LAC than that of  $Er_2O_3$  and the lowest LAC is found for the glass with  $Ho_2O_3$ . This is related to the atomic numbers of the elements Ho, Er and Tm ( $Z = 67, 68$  and  $69$  respectively).

It is deserved investigating the radiation attenuation competence for the chosen glasses in terms of half value layer (HVL) [35]. It denotes the thickness of the medium that reduces the incoming radiation to 50% of its actual intensity. The theoretical determination of HVL for the chosen samples can be achieved from the LAC using  $HVL = 0.693/LAC$ . The HVL curves for the fabricated glasses are plotted in Fig. 7. Before examining the curves, one must keep in mind that for advantageous protection material, smaller HVL is recommended. In this case, the number of gamma photons interacting with the protection material is high and hence the



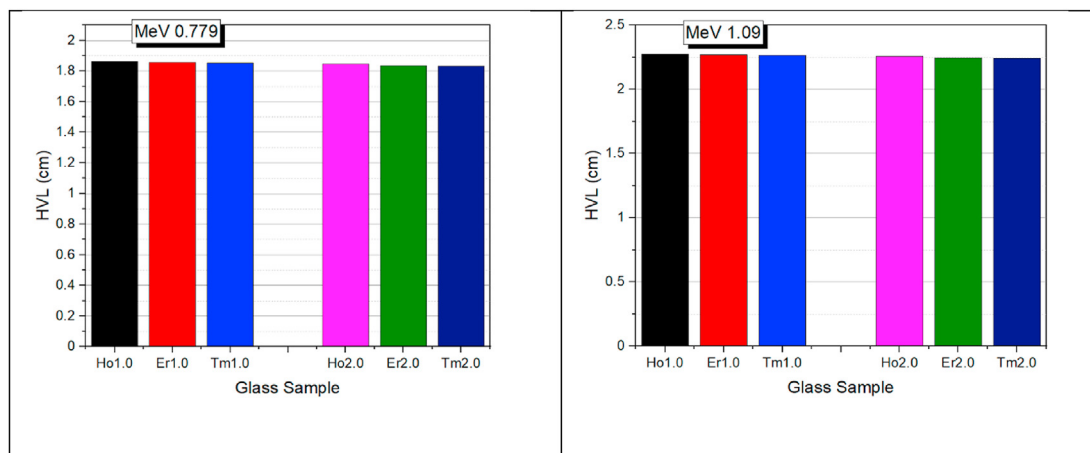


Fig. 8. Half value layer for the Ho1.0, Er1.0 and Tm1.0 (and for the samples with 2 mol% of Rare earth ions) at 0.779 and 1.09 MeV.

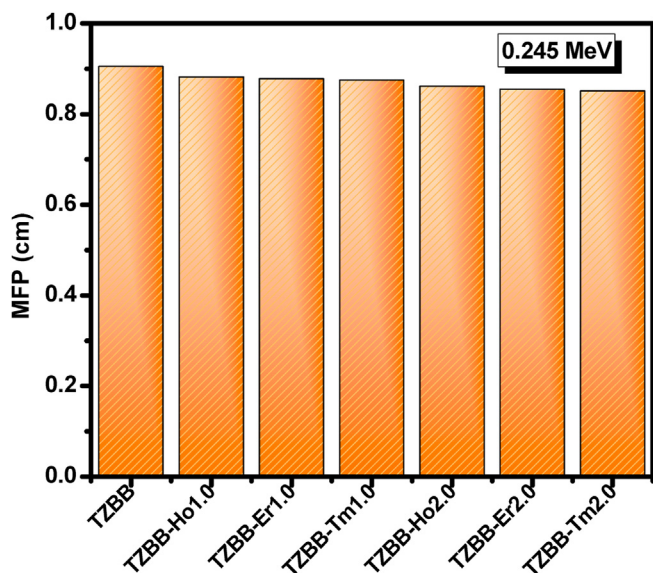


Fig. 9. Mean free path (cm) for the fabricated glasses at 0.245 MeV.

attenuation is also high. Clearly, HVL increases with increasing energy and reaches a maximum value at 1.01 MeV and equals to 2.322 cm for TZBB glass. On contrast, the minimum HVL is reported at 0.245 MeV and equals to 0.627 cm for TZBB glass. The addition of Ho<sub>2</sub>O<sub>3</sub> decreases the HVL and both samples TZBB-Ho1.0 and TZBB-Ho2.0 have lowest HVL than the TZBB. The addition of Ho<sub>2</sub>O<sub>3</sub> by 2 mol% leads to decrease of the HVL from 0.984 cm (for TZBB) to 0.948 cm (for TZBB-Ho2.0) at 0.344 MeV and from 1.743 cm to 1.705 cm at 0.689 MeV. At all the investigated energies, the addition of Ho<sub>2</sub>O<sub>3</sub> reduces the HVL and thus the rare earth ions doped glasses have better shielding performance than TZBB glass. Similar result is found for both Er<sub>2</sub>O<sub>3</sub> and Tm<sub>2</sub>O<sub>3</sub>.

In Fig. 8, we plotted the HVL for the three glasses TZBB-Ho1.0, TZBB-Er1.0 and TZBB-Tm1.0 at 0.779 and 1.09 MeV. Also, we included the HVL for the samples with 2 mol% of the rare earth ions. The aim of this figure is to compare the influence of Ho<sub>2</sub>O<sub>3</sub>, Er<sub>2</sub>O<sub>3</sub> and Tm<sub>2</sub>O<sub>3</sub> on the HVL values. Apparently, the HVL follows the following trend: TZBB-Tm1.0 < TZBB-Er1.0 < TZBB-Ho1.0, and TZBB-Tm2.0 < TZBB-Er2.0 < TZBB-Ho2.0. This is also correct for the other energies, but only the comparison at 0.779 and 1.09 MeV is

presented. From this result, TZBB-Tm2.0 is found to be the best attenuator among the glasses chosen in this investigation. Also, as we found in the LAC curves, all the samples with rare earth ions have better HVL and thus shielding competence than TZBB.

The gamma shielding properties of the TZBB glass and the glasses with Ho<sub>2</sub>O<sub>3</sub>, Er<sub>2</sub>O<sub>3</sub> and Tm<sub>2</sub>O<sub>3</sub> are discussed using the concept of the mean free path (MFP). We plotted the MFP for the fabricated glasses at 0.245 MeV in Fig. 9. A notable decrease is observed with addition of rare earth ions. Apparently, TZBB has lower MFP than other glasses. For TZBB, the MFP is 0.905 cm, and this decreased to 0.882 cm due to the addition of Ho<sub>2</sub>O<sub>3</sub> by 1 mol%, and to 0.878 cm due to adding 1 mol% of Er<sub>2</sub>O<sub>3</sub> and to 0.875 cm due to adding 1 mol% of Tm<sub>2</sub>O<sub>3</sub>. This result is in line with the results obtained in the previous curves namely, the glass with Tm<sub>2</sub>O<sub>3</sub> has lower MFP than that of Er<sub>2</sub>O<sub>3</sub> followed by Ho<sub>2</sub>O<sub>3</sub>. Also, adding 2 mol% of each of these rare earth ions leads to more reduction in the MFP.

#### 4. Conclusions

One and two mol.% of thulium, erbium and holmium doped barium tellurite glasses were investigated for their physical, structural and radiation shielding properties. Owing to the mass differences of dopant atoms, thulium doped glasses had highest density and least molar volume. Bandgap value of 3.615 eV obtained for barium tellurite glass was found to get altered owing to rare earth dopant addition, which along with Raman spectral results indicated structural modifications occurring in the network. Rare earth doped glasses were found to show higher linear attenuation coefficient values compared to base barium tellurite glass and has been correlated to photoelectric mechanism or Compton scattering depending on the range of energies. Among all the investigated glasses for radiation shielding properties, thulium doped glasses were found to be having highest linear attenuation coefficient value of 1.18 cm<sup>-1</sup> at 0.245 MeV for 2 mol.% doping compared to all other glasses. Similarly, mean free path and half value layer of 2 mol.% thulium doped showed the least values indicating these are better attenuators among all the investigated glasses.

#### Declaration of competing interest

The authors declare that they have no known competing financial interests or personal relationships that could have appeared to influence the work reported in this paper.

## Acknowledgments

One of the authors (NM) wishes to thank SERB-DST for financial support through project grant SB/S2/LOP-013 for executing part of this work.

## References

- [1] S. Yasmin, B.S. Barua, Khandaker Mu, Rashid Ma, D.A. Bradley, Olatunji Ma, M. Kamal, Studies of ionizing radiation shielding effectiveness of silica-based commercial glasses used in Bangladeshi dwellings, *Respir. Physiol.* 9 (2018) 541–549.
- [2] Erdem Şakar, Özpolat Özgür Fırat, M.I. Bünyamin Alım, Sayyed, M. Kurudirek, Phy-X/PSD: development of a user-friendly online software for calculation of parameters relevant to radiation shielding and dosimetry, *Radn. Phys. Chem.* 166 (2020) 108496.
- [3] M.I. Sayyed, Julius Federico M. Jecong, Frederick C. Hila, Charlotte V. Balderas, Abdullah M.S. Alhuthali, Neil Raymond D. Guillermo, Yas Al-Hadeethi, Radiation shielding characteristics of selected ceramics using the EPICS2017 library, *Ceram. Int.* 47 (2021) 13181.
- [4] Nadin Jamal, Abu Al Roos, Noorfatin Aida Baharul Amin, Rafidah Zainon Conventional and new lead-free radiation shielding materials for radiation protection in nuclear medicine: a review, *Radn. Phys. Chem.* 165 (2019) 108439.
- [5] Mengge Dong, Xiangxin Xue, Yang He, Zhefu Li, Highly cost-effective shielding composite made from vanadium slag and boron-rich slag and its properties, *Radn. Phys. Chem.* 141 (2017) 239–244.
- [6] B.O. Elbashir, M.G. Dong, M.I. Sayyed, Shams A.M. Issa, K.A. Matori, M.H.M. Zaid, Comparison of Monte Carlo simulation of gamma ray attenuation coefficients of amino acids with XCOM program and experimental data, *Results Phys.* 9 (2018) 6–11.
- [7] Mengge Dong, Suying Zhou, Xiangxin Xue, Xiating Feng, M.I. Sayyed, Mayeen Uddin Khandaker, D.A. Bradley, The potential use of boron containing resources for protection against nuclear radiation, *Radn. Phys. Chem.* 188 (2021) 109601, 045303.
- [8] M.I. Sayeed, Y. Al-Hadeethi, Maha M. AlShammari, M. Ahmed, S.H. Al-Heniti, Y.S. Hammah, Physical, optical and gamma radiation shielding competence of newly boro-tellurite based glasses: TeO<sub>2</sub>–B<sub>2</sub>O<sub>3</sub>–ZnO–Li<sub>2</sub>O<sub>3</sub>–Bi<sub>2</sub>O<sub>3</sub>, *Ceram. Int.* 47 (2021) (2021) 611.
- [9] Aljawhara H. Almuqrin, M.I. Sayyed, Radiation shielding characterizations and investigation of TeO<sub>2</sub>–WO<sub>3</sub>–Bi<sub>2</sub>O<sub>3</sub> and TeO<sub>2</sub>–WO<sub>3</sub>–PbO glasses, *Appl. Phys. A* 127 (2021) 190.
- [10] P. Vani, G. Vinitha, M.I. Sayyed, B.O. El Bashir, N. Manikandan, Investigation on structural, optical, thermal and gamma photon shielding properties of zinc and barium doped fluorotellurite glasses, *J. Non-Cryst. Sol.* 511 (2019) 194.
- [11] M.I. Sayyed, Aljawhara H. Almuqrin, Recep Kurtulus, Abigaile Mia V. Javier-Hila, Kawa Kaky, Taner Kavas, X-ray shielding characteristics of P<sub>2</sub>O<sub>5</sub>–Nb<sub>2</sub>O<sub>5</sub> glass doped with Bi<sub>2</sub>O<sub>3</sub> by using EPICS2017 and Phy-X/PSD, *Appl. Phys. A* 127 (2021) 243.
- [12] G. Lakshminarayana, Ashok Kumar, A. Lira, A. Dahshan, H.H. Hegazy, V. Kityk, Eun Lee Dong, Jonghun Yoon, Taejoon Park, Comparative study of gamma-ray shielding features and some properties of different heavy metal oxide-based tellurite-rich glass systems, *Radn. Phys. Chem.* 170 (2020) 108633.
- [13] M.I. Sayeed, Shams A.M. Issa, Mehmet Buyukyildiz, M. Dong, Determination of nuclear radiation shielding properties of some tellurite glasses using MCNP5 code, *Radn. Phys. Chem.* 150 (2018) 1.
- [14] M.I. Sayyed, K.A. Mahmoud, O.L. Tashlykov, Mayeen Uddin Khandaker, M.R.I. Faruque, Enhancement of the shielding capability of soda–lime glasses with Sb<sub>2</sub>O<sub>3</sub> dopant: a potential material for radiation safety in nuclear installations, *Appl. Sci.* 11 (2021) 326.
- [15] M.I. Sayyed, K.A. Mahmoud, E. Lacomme, Maha M. AlShammari, Nidal Dwaikat, Y.S.M. Alajerami, Muna Alqahtani, B.O. El-bashir, M.H.A. Mhareb, Development of a novel MoO<sub>3</sub>-doped borate glass network for gamma-ray shielding applications, *Eur. Phys. J. Plus* 136 (2021) 108.
- [16] Preet Kaur, Devinder Singh, Tejbir Singh, Heavy metal oxide glasses as gamma rays shielding material, *Nucl. Eng. Des.* 307 (2016) 364.
- [17] M.I. Sayyed, Aljawhara H. Almuqrin, Ashok Kumar, J.F.M. Jecong, I. Akkurt, Optical, mechanical properties of TeO<sub>2</sub>–CdO–PbO–B<sub>2</sub>O<sub>3</sub> glass systems and radiation shielding investigation using EPICS2017 library, *Optik* 242 (2021) 167342.
- [18] M.S. Al-Buriahi, C. Sriwunkum, Halil Arslan, Baris T. Tongue, Mohamed A. Bourham, Investigation of barium borate glasses for radiation shielding applications, *Appl. Phys. A* 126 (1) (2020) 68.
- [19] R. El-Mallawany, W.M. Abou-Taleb, M.A. Naeem, M.E. Krar, S. Talaat, Synthesis, physical, optical properties and gamma-ray shielding parameters of some tellurite glasses, *Optik* 242 (2021) 167171.
- [20] N. Manikandan, Aleksandr Ryasnyanskiy, Jean Toulouse, Thermal and optical properties of TeO<sub>2</sub>–ZnO–BaO glasses, *J. Non-Cryst. Sol.* 358 (2012) 947.
- [21] K. Boonin, P. Yasaka, P. Limkitjaroenporn, R. Rajaramakrishna, A. Askin, M.I. Sayyed, S. Kothan, J. Kaewknao, Effect of BaO on lead free zinc barium tellurite glass for radiation shielding materials in nuclear materials, *J. Non-Cryst. Sol.* 550 (2020) 120386.
- [22] Jie Li, Xusheng Xiao, Shaoxuan Gu, Yantao Xu, Zhiguang Zhou, Haitao Guo, Preparation and optical properties of TeO<sub>2</sub>–BaO–ZnO–ZnF<sub>2</sub> fluoro-tellurite glass for mid-infrared fiber Raman laser applications, *Opt. Mater.* 66 (2017) 567.
- [23] Kh A. Bashar, G. Lakshminarayana, S.O. Baki, Al-B.F.A. Mohammed, U. Caldino, A.N. Meza Rocha, Vijay Singh, I.V. Kityk, M.A. Mahdi, Tunable white-light emission from Pr<sup>3+</sup>/Dy<sup>3+</sup> co-doped B<sub>2</sub>O<sub>3</sub>–TeO<sub>2</sub>–PbO–ZnO–Li<sub>2</sub>O–Na<sub>2</sub>O glasses, *Opt. Mater.* 88 (2019) 558.
- [24] F.I. El-Agawany, E. Kavaz, U. Perisanoglu, M. Al-Buriahi, Y.S. Rammah, Sm<sub>2</sub>O<sub>3</sub> effects on mass stopping power/projected range and nuclear shielding characteristics of TeO<sub>2</sub>–ZnO glass systems, *Appl. Phys. A* 125 (2019) 838.
- [25] Al-Hadeethi, M. Ahmed, Saleh H. Al-Heniti, M.I. Sayyed, Y.S. Rammah, Rare earth Co-Doped tellurite glass ceramics: potential use in optical and radiation shielding applications, *Ceram. Int.* 46 (2020) 19198.
- [26] Y.S. Rammah, M.I. Sayyed, B.O. El Bashir, S.M. Asiri, Y. Al-Hadeethi, Linear optical features and radiation shielding competence of ZnO–B<sub>2</sub>O<sub>3</sub>–TeO<sub>2</sub>–Eu<sub>2</sub>O<sub>3</sub> glasses: role of Eu<sup>3+</sup> ions, *Opt. Mater.* 111 (2021) 110525.
- [27] S.A. Tijani, S.M. Kamal, Y. Al-Hadeethi, M. Arib, M.A. Hussein, S. Wageh, L.A. Dim, Radiation shielding properties of transparent erbium zinc tellurite glass system determined at medical diagnostic energies, *J. Alloys. Cpd.* 741 (2018) 293.
- [28] M.S. Al-Buriahi, I.O. Olarinoye, Sultan Alomairy, Imen Kebaili, Rumeysa Kaya, Halil Arslan, Baris T. Tongue, Dense and environment friendly bismuth barium telluroborate glasses for nuclear protection applications, *Prog. Nucl. Energy* 137 (2021) 103763.
- [29] M.K. Halimah, L. Hasnimulyati, A. Zakaria, S.A. Halim, M. Ishak, A. Azuraida, N.M. Al-Hada, et al., Influence of gamma radiation on the structural and optical properties of thulium-doped glass, *Mater. Sci. Eng. B* 226 (2017) 158.
- [30] N.F. Mott, E.A. Davis, *Electronic Process in Non-crystalline Materials*, 1971.
- [31] J. Tauc, F. Abeles (Eds.), *Optical Properties of Solids*, North Holland, Amsterdam, 1969, p. 227.
- [32] K. Aishwarya, G. Vinitha, G. Sreevidya Verma, S. Asokan, N. Manikandan, Synthesis and characterization of barium fluoride substituted zinc tellurite glasses, *Physica B* 526 (2017) 84.
- [33] R.T. Alves, A.C.A. Silva, N.O. Dantas, A.S. Gouveia-Neto, Raman and optical spectroscopy studies in Tm<sup>3+</sup>/Dy<sup>3+</sup> co doped zinc tellurite glasses, *J. Lumin.* 230 (2021) 117738.
- [34] S. Kaewjaeng, S. Kothan, W. Chaiphaksa, N. Chanthima, R. Rajaramakrishna, H.J. Kim, J. Kaewkhaio, High transparency La<sub>2</sub>O<sub>3</sub>–CaO–B<sub>2</sub>O<sub>3</sub>–SiO<sub>2</sub> glass for diagnosis x-rays shielding material application, *Radiat. Phys. Chem.* 160 (2019) 41.
- [35] M.I. Sayyed, M.H.A. Mhareb, Y.S.M. Alajerami, K.A. Mahmoud, Mohammad A. Imheidat, Fatimh Alshahri, Muna Alqahtani, T. Al-Abdullah, Optical and radiation shielding features for a new series of borate glass samples, *Optik* 239 (2021) 166790.
- [36] M.I. Sayyed, O.I. Olarinoye, Elsafi Mohamed, Assessment of gamma-radiation attenuation characteristics of Bi<sub>2</sub>O<sub>3</sub>–B<sub>2</sub>O<sub>3</sub>–SiO<sub>2</sub>–Na<sub>2</sub>O glasses using Geant4 simulation code, *Eur. Phys. J. Plus* 136 (2021) 535.